phys. stat. sol. (b) **219**, 23 (2000)

Subject classification: 68.60.Wm; 78.70.–g; S5

Electronic Stopping Power of Amorphous Carbon for H_2^+ and H_3^+ Beams

R. GARCIA-MOLINA (a), C. D. DENTON[1]) (a), F. J. PÉREZ-PÉREZ (b), I. ABRIL (c), and N. R. ARISTA (d)

(a) Departamento de Física, Universidad de Murcia, Apartado 4021, E-30080 Murcia, Spain

(b) School of Physical and Mathematical Sciences, Loughborough University, Loughborough LE11 3TU, U.K.

(c) Departament de Física Aplicada, Universitat d'Alacant, Apartat 99, E-03080 Alacant, Spain

(d) Instituto Balseiro, Centro Atómico Bariloche, RA-8400 Bariloche, Argentina

(Received November 22, 1999; in revised form February 11, 2000)

The electronic stopping power of amorphous carbon targets for H_2^+ and H_3^+ molecular beams has been analysed within the framework of the dielectric formalism. Coulomb explosion between the partners of the molecule has been taken into account to evaluate the average stopping power ratio during the dwell time. The charge state of the fragments is assumed fully stripped. Analysis and comparison of the calculated stopping power ratio with experimental data show a reasonable agreement.

1. Introduction

Experimental results of fast molecular ion beams interacting with thin foils have revealed the presence of vicinage (or interference) effects that occur when two or more particles travel in correlated motion through a solid. These vicinage effects between molecular partners may produce an enhancement or a diminution of the slow down of the correlated particles when compared to that of an isolated projectile; this effect is caused by the interference of the electronic excitations induced in the target by the components of the molecule. The first experimental evidence of the vicinage effects was observed by Brandt et al. [1] with molecular beams of H_2^+ and H_3^+, and after that, several papers have been devoted to its study. Most of the experimental [2 to 10] and theoretical [11 to 13] works have chosen H_2^+ and H_3^+ as molecular projectiles because they have the simplest structure where vicinage effects can be observed: H_2^+ is a molecule with a mean internuclear distance equal to 2.4 a.u. [14], and H_3^+ is an equilateral triangular molecule with sides of 1.9 a.u. [15]. Therefore it is interesting to evaluate the vicinage effects for these molecular beams because they depend on the geometrical configuration and velocity of the molecule as well as on the target properties.

The purpose of this paper is to compare the theoretical predictions obtained by our model with the available experimental data for the stopping power of amorphous car-

[1]) Permanent address: Instituto Balseiro, Centro Atómico Bariloche, RA-8400 Bariloche, Argentina

bon for H_2^+ and H_3^+ molecular beams. This model takes into account the spatial changes of the initial configuration of the protons in the molecule, due to Coulomb explosion, and it uses the dielectric formalism to evaluate the electronic energy loss and the interference effects of the particles that constitute the molecule [13]. The dielectric properties of the amorphous carbon target are described by a sum of Mermin-type energy loss function [17]. In this scheme we find the electronic energy loss of the H_2^+ and H_3^+ molecular beams after traversing the foil as the averaged instantaneous energy loss over the dwell time. A random orientation of the incident molecules is chosen in order to compare with the experimental situation. A detailed study of the role played by the different molecular orientations in the energy loss of fast H_3^+ is given in Refs. [18, 19].

2. Model

For a complete description of the interaction between the molecular beam and the target, it is necessary to consider the changes that occur on the projectile during its path through the foil. When a fast H_2^+ or H_3^+ molecule interacts with a solid, its binding electrons are usually stripped off in the first atomic layers and the molecule becomes a set of protons with the structure of the molecule, which move in correlated motion; during this motion, their internuclear separation increases due to Coulomb repulsion.

The nuclear energy loss can be neglected in the range of energies we shall consider. The dielectric formalism provides an expression for the instantaneous electronic stopping power of a solid, S_N^{inst}, corresponding to N protons that travel in correlated motion with velocity v, as a function of the instantaneous separation r between the particles [20],

$$S_N^{\text{inst}}(r) = \left[\sum_{i=1}^{N} Z_i^2 + \sum_{i\neq j}^{N} Z_i Z_j I(r)\right] S_{\text{p}}\,, \tag{1}$$

where S_{p} is the stopping power of the target for a single proton, $I(r)$ is the vicinage function, and Z_i represents the charge of each particle. The first term in Eq. (1) represents the contribution to the stopping power of the target from each proton of the molecule, while the second term takes into account the interference effects that appear due to the proximity of the proton partners. Atomic units will be used throughout this paper[2]), and we assume that the charge of each fragment proton in correlated motion does not differ from that of an isolated proton, so $Z_i = Z_j = 1$.

According to the dielectric formalism, the electronic stopping power of a solid for a proton moving with velocity v is

$$S_{\text{p}} = \frac{2}{\pi v^2} \int_0^{\infty} \frac{\mathrm{d}k}{k} \int_0^{kv} \mathrm{d}\omega\, \omega\, \text{Im}\left[\frac{-1}{\epsilon(k,\omega)}\right]. \tag{2}$$

The response of the solid to the passage of the charged projectile is contained in the term $\text{Im}[-1/\epsilon(k,\omega)]$, the so called energy loss function (ELF); k and ω are, respectively, the momentum and energy transferred into electronic excitations to the target electrons.

[2]) Atomic units are defined by the condition $m_{\text{e}} = e = \hbar = 1$, where m_{e} is the mass of the electron and e is the elementary charge.

Table 1
Parameters used to fit the energy loss function (ELF) of amorphous carbon using Eq. (4)

j	ω_j (a.u.)	γ_j (a.u.)	A_j
1	0.230	0.21	0.2362
2	0.945	0.49	0.7088

$i-$ shell	$\omega_{i-\text{shell}}$ (a.u.)	$\gamma_{i-\text{shell}}$ (a.u.)	$A_{i-\text{shell}}$	$\omega_{i-\text{edge}}$ (a.u.)
K	10.5	7.9	0.004078	10.4

The vicinage function, $I(r)$, incorporates the interference effects between the correlated protons. For a random orientation of the molecule, it is given by [18]

$$I(r) = \frac{2}{\pi v^2 S_\text{p}} \int_0^\infty \frac{\text{d}k}{k} \frac{\sin kr}{kr} \int_0^{kv} \text{d}\omega\, \omega\, \text{Im}\left[\frac{-1}{\epsilon(k,\omega)}\right]. \tag{3}$$

We consider two main contributions to the energy loss function: one due to the valence electrons ($\omega < \omega_{i-\text{edge}}$), and the other from the inner electrons ($\omega \geq \omega_{i-\text{edge}}$) of the target atoms, where $\omega_{i-\text{edge}}$ is the threshold energy of the i-shell. The ELF of the target is constructed by a sum of Mermin-type ELF fitted to the structure of the experimental ELF at $k = 0$ (optical data) [16, 17],

$$\text{Im}\left[\frac{-1}{\epsilon(k=0,\omega)}\right]_\text{experim} = \begin{cases} \sum_j A_j\, \text{Im}\left[\dfrac{-1}{\epsilon_\text{M}\,(k=0,\omega;\omega_j,\gamma_j)}\right] & \text{if} \quad \omega < \omega_{i-\text{edge}} \\ \sum\limits_{i-\text{shell}} A_{i-\text{shell}}\, \text{Im}\left[\dfrac{-1}{\epsilon_\text{M}\,(k=0,\omega;\omega_{i-\text{shell}},\gamma_{i-\text{shell}})}\right] & \text{if} \quad \omega \geq \omega_{i-\text{edge}}\,, \end{cases} \tag{4}$$

where ϵ_M is the Mermin dielectric function [21]; ω_j, γ_j and A_j describe, respectively, the positions, widths and heights of the ELF peaks for the valence electrons. The values of $\omega_{i-\text{shell}}$, $\gamma_{i-\text{shell}}$ and $A_{i-\text{shell}}$ are chosen to fit the shape of the ELF in the corresponding inner shells. The coefficients A_j and $A_{i-\text{shell}}$ are determined under the requirement that the f-sum rule for the effective number of target electrons participating in the electronic excitations must be satisfied [17]. The parameters of the ELF for an amorphous carbon target are presented in Table 1. The contribution of the valence electrons to the ELF was fitted, at $k = 0$, by a sum of two Mermin-type ELF to the experimental data [22], while the contribution of the K-inner shell was deduced from X-ray scattering factors [23][3]).

For a given internuclear distance r between proton fragments, the instantaneous stopping power ratio

$$R_N^\text{inst}(r) = \frac{S_N^\text{inst}(r)}{N S_\text{p}} \tag{5}$$

[3]) The ASCII files for the X-ray scattering factors of the different elements can be obtained from http://xray.uu.se/hypertext/henke.html.

compares the energy loss of N correlated protons with N times the energy loss of a single proton, in the same material and at the same velocity. If this ratio is equal to unity, then there are not interference effects. Values of $R_N^{\text{inst}} > 1$ (or < 1) represent an enhancement (or a diminution) of the molecular energy loss with respect to that of a single proton.

In order to make a comparison with experimental results, we evaluate the total energy lost by the molecule during its path inside the target, along which the internuclear distance grows due to the Coulomb explosion. The measured stopping power ratio is the average of the instantaneous stopping power ratio over the dwell time τ

$$R_N^{\text{aver}} = \frac{1}{\tau} \int_0^{\tau} \mathrm{d}t \; R_N^{\text{inst}}(r(t)) \,. \tag{6}$$

In a good approximation, the dwell time can be calculated as $\tau = D/v$, where D is the foil thickness.

The interaction between the proton fragments separated by a internuclear distance r is described by the screened Coulomb potential [24]

$$V(r) = \frac{\mathrm{e}^{-r/a}}{r} \,, \tag{7}$$

where a is the screening length, given by $a = v/\omega_{\text{pl}}$ when $v > v_{\text{F}}$ and $a = v_{\text{F}}/\omega_{\text{pl}}$ otherwise; $v_{\text{F}} = 1.2$ a.u. and $\omega_{\text{pl}} = 0.8$ a.u. are, respectively, the Fermi velocity and the characteristic plasmon energy of the material. Solving the coupled set of Newton equations for the components of the molecule that feel the screened Coulomb potential, we obtain the instantaneous distance between the protons as a function of the time, $r(t)$. Note that the effect of the Coulomb repulsion in the H_3^+ molecule is to increase each side of the equilateral triangle without changing its shape.

3. Results and Discussion

In Fig. 1 we present the average stopping power ratio R_2^{aver} of amorphous carbon for H_2^+, as a function of the dwell time and for constant values of the foil thickness. A comparison between experiments (symbols) and theoretical results (lines) is shown for several thicknesses: 2 μg/cm^2 [5], 3 μg/cm^2 [3, 8], 5 μg/cm^2 [4, 5], 6 μg/cm^2 [8] and 10.5 μg/cm^2 [4, 8]. The dwell time τ was chosen as parameter in order to include in the same figure different experimental results. The vicinage effects in the stopping power are more pronounced at low dwell times, when the internuclear distance has not grown yet too much due to Coulomb explosion. At long dwell times (corresponding to smaller velocities and/or thicker foils) R_2^{aver} goes to unity because the molecular partners have enough time to separate, and the protons travel without mutual interaction for longer times. The theoretical calculation of the stopping power ratio shows a reasonable agreement with the experimental data (within the error bars), especially at large foil thicknesses; the difficulty to characterise the foils (density and homogeneity) could explain the poorer agreement at small thicknesses. For small velocities and foil thicknesses, the model does not predict values of the stopping power ratio lower than unity, as seen in some of the experimental data. This feature could be explained because in our calculation we have not considered that, once in the material, the mole-

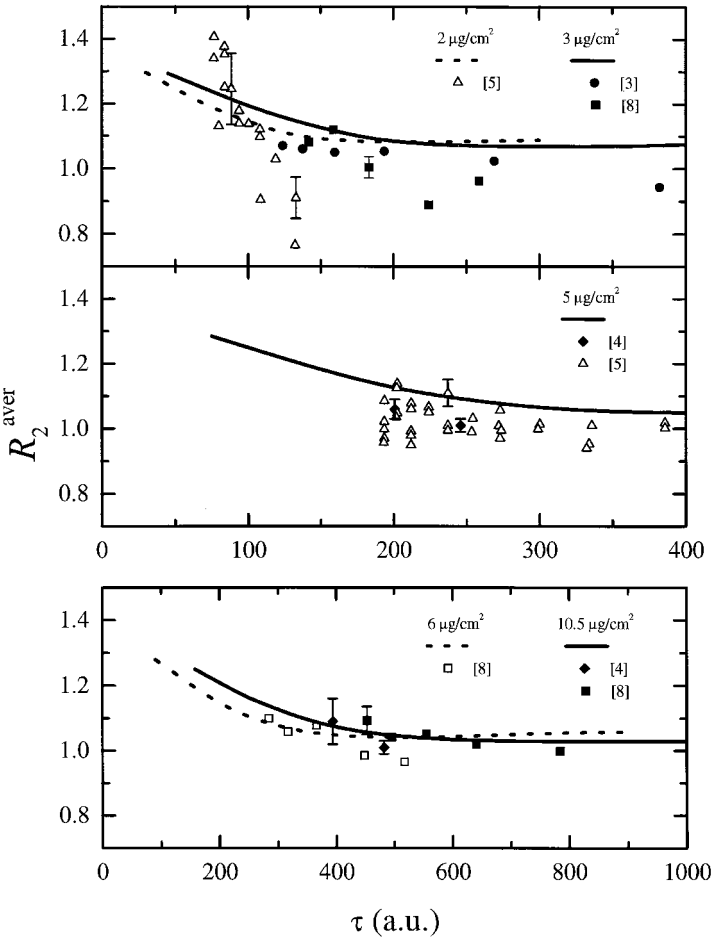

Fig. 1. R_2^{aver} for H_2^+ molecular beams in amorphous carbon foils, as a function of the dwell time. Different thicknesses are considered: 2, 3, 5, 6 and 10.5 μg/cm^2. Lines correspond to our calculations, and experimental data are represented by symbols (as indicated in each part)

cular fragments tend to become aligned parallel to the velocity, due to the wake force induced by the leading projectile [17]. Calculations made for incident aligned molecules show that $R_2^{aver} < 1$ at low velocities.

Figure 2 displays the stopping power ratio R_2^{aver} of amorphous carbon for H_2^+, as a function of the dwell time and for constant energies of the H_2^+ molecular beam. Experimental data from different authors [1 to 8] with energies ranging from 12.25 to 1000 keV/amu are presented here. Again it can be seen that the interference effects are more pronounced at low dwell times and go to unity at large dwell times. This tendency to unity is slower at high velocities due to the larger extension of the interference wake potential. Generally the agreement of our calculations with the experimental data is reasonable (taking into account the variety of analysed experiments), except in the case of the data from Ref. [6], corresponding to ultrathin targets and low velocities. A large

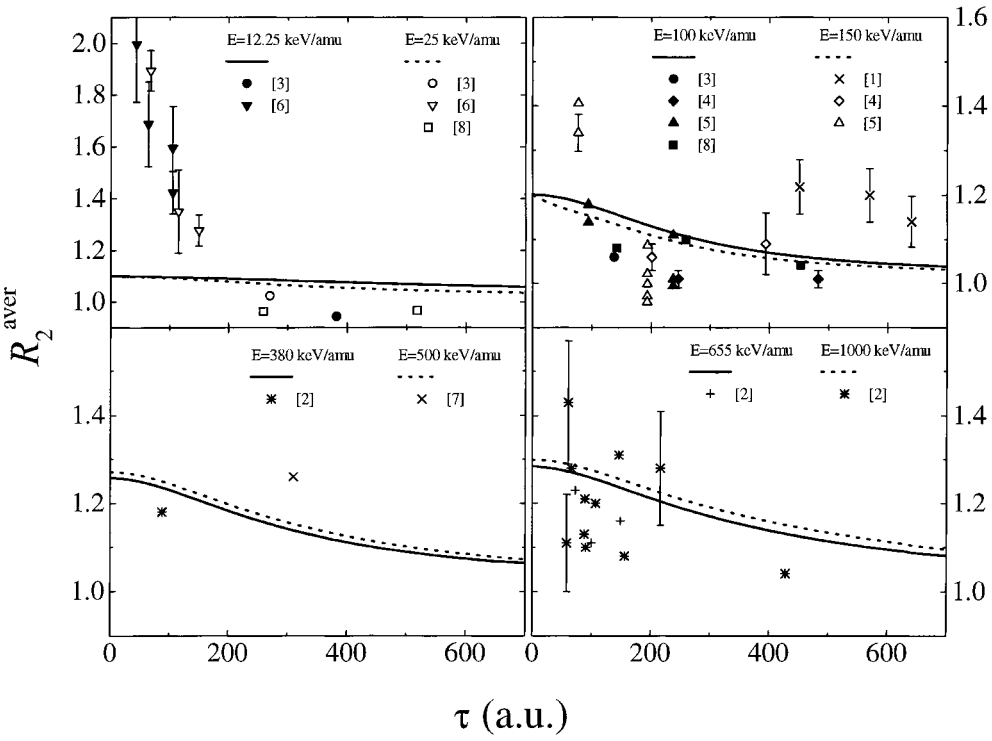

Fig. 2. R_2^{aver} for H_2^+ molecular beams in amorphous carbon foils, as a function of the dwell time. Different energies are considered: 12.25, 25, 100, 150, 380, 500, 655 and 1000 keV/amu. Lines correspond to our calculations, and experimental data are represented by symbols (as indicated in each part)

dispersion of the experimental data from different authors is observed, and a tendency in the dependence of the stopping power ratio with the foil thickness or the energy is not obvious from these data. Further and more accurate measurements of this quantity would be desirable.

Figure 3 shows experimental data and theoretical predictions for the stopping power ratio R_3^{aver} of amorphous carbon for a H_3^+ molecule, as a function of the dwell time. Our calculations correspond to the experimental data reported by Ray et al. [8] for three foil thicknesses (3, 6 and 10.5 μg/cm^2); a single experimental data from Nyaiesh et al. [4] for a 5 μg/cm^2 thickness is included for completeness. The stopping power ratio for H_3^+ molecular beams shows the same behaviour as for H_2^+ molecules (see Fig. 1). In all the cases analysed, the results show values of the stopping power ratio greater than one. For small dwell times the stopping power ratio goes to the same value, independent of the foil thickness. At long dwell times, or small energies, the stopping power ratio approaches to unity because the molecular fragments have enough time to become separated. The main difference between the stopping power ratios occurs at small dwell times, where $R_3^{aver} > R_2^{aver}$. The enhancement of the vicinage effects in the case of H_3^+ is because its protons are initially closer than in H_2^+.

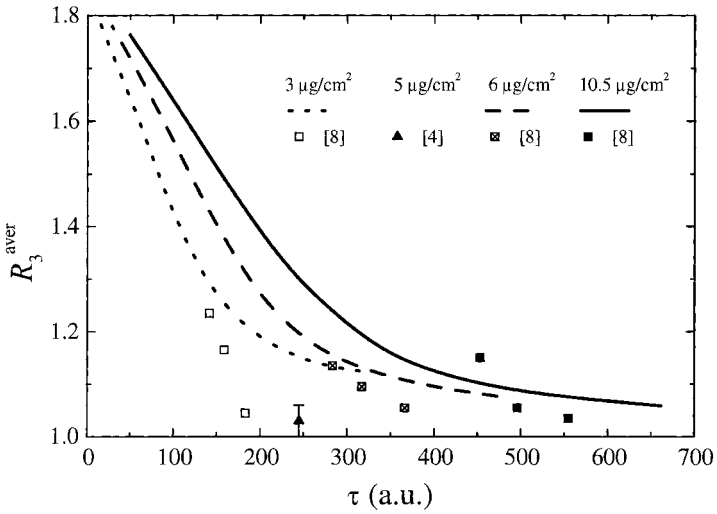

Fig. 3. R_3^{aver} for H_3^+ molecular beams in amorphous carbon foils, as a function of the dwell time. Different thicknesses are considered: 3, 5, 6 and 10.5 μg/cm^2. Symbols correspond to experimental data from Nyaiesh et al. [4] and Ray et al. [8]. Lines represent our calculations

4. Conclusions

We have calculated the stopping power ratio of amorphous carbon for H_2^+ and H_3^+ molecules, using the dielectric formalism and taking into account the Coulomb explosion between the protons of the molecule. This quantity has been evaluated as a function of the dwell time, for different foil thicknesses and molecular beam energies. Both stopping power ratios, R_2^{aver} and R_3^{aver}, show the same trend as a function of the dwell time, with the stopping ratio for H_3^+ being greater than that for H_2^+ at small dwell times. Despite the dispersion of experimental data, our results compare reasonably well with them, reproducing their main features.

Acknowledgements We acknowledge partial support from the Spanish DGICYT (project PB96-1118) and from the Generalitat Valenciana (project GV99-54-1-01). C.D.D. thanks the Fundación Séneca (Comunidad Autónoma de la Región de Murcia) for financial support.

References

[1] W. Brandt, A. Ratkowski, and R. H. Ritchie, Phys. Rev. Lett. **33**, 1325 (1974).
[2] J. W. Tape, W. M. Gibson, J. Remillieux, R. Laubert, and H. E. Wegner, Nucl. Instrum. Methods **132**, 75 (1976).
[3] J. C. Eckardt, G. Lantschner, N. R. Arista, and R. A. Baragiola, J. Phys. C **11**, L851 (1978).
[4] A. R. Nyaiesh, W. Steckelmacher, and M. W. Lucas, J. Phys. C **11**, 2917 (1978).
[5] R. Laubert, IEEE Trans. Nucl. Sci. **26**, 1020 (1979).
[6] R. Levi-Setti, K. Lam, and T. R. Fox, Nucl. Instrum. Methods **194**, 281 (1982).
[7] Y. Horino, M. Renda, and K. Morita, Nucl. Instrum. Methods B **33**, 178 (1988).
[8] E. Ray, R. Kirsch, H. M. Mikkelsen, J. C. Poizat, and J. Remillieux, Nucl. Instrum. Methods B **69**, 133 (1992).
[9] Y. Susuki, T. Ito, K. Kimura, and M. Mannami, Nucl. Instrum. Methods B **61**, 3535 (1992).

[10] M. FRITZ, K. KIMURA, Y. SUSUKI, and M. MANNAMI, Phys. Rev. A **50**, 2405 (1994).
[11] T. KANEKO, Phys. Rev. A **51**, 535 (1995).
[12] M. M. JAKAS and N. E. CAPUJ, J. Phys.: Condensed Matter **5**, 4593 (1995).
[13] C. D. DENTON, F. J. PÉREZ-PÉREZ, I. ABRIL, R. GARCIA-MOLINA, and N. R. ARISTA, Europhys. Lett. **35**, 499 (1996).
[14] W. L. WALTERS, D. G. COSTELLO, J. G. SKOFRONICK, D. W. PALMER, W. E. KANE, and R. G. HERB, Phys. Rev. **125**, 2012 (1962).
[15] M. J. GAILLARD, D. S. GEMMELL, G. GOLDRING, I. LEVINE, W. J. PIETSCH, J.-C. POIZAT, A. J. RATKOWSKI, J. REMILLIEUX, Z. VAGER, and B. J. ZABRANSKY, Phys. Rev. A **17**, 1797 (1978).
[16] D. J. PLANES, R. GARCIA-MOLINA, I. ABRIL, and N. R. ARISTA, J. Electron Spectroscopy Relat. Phenom. **82**, 23 (1996).
[17] I. ABRIL, R. GARCIA-MOLINA, C. DENTON, F. J. PÉREZ-PÉREZ, and N. R. ARISTA, Phys. Rev. A **58**, 357 (1998).
[18] C. D. DENTON, I. ABRIL, F. J. PÉREZ-PÉREZ, R. GARCIA-MOLINA, and N. R. ARISTA, Radiat. Eff. Def. Sol. **142**, 223 (1997).
[19] F. J. PÉREZ-PÉREZ, C. D. DENTON, I. ABRIL, R. GARCIA-MOLINA, and N. R. ARISTA, Z. Phys. D **41**, 187 (1997).
[20] N. R. ARISTA, Phys. Rev. B **18**, 1 (1978).
[21] N. D. MERMIN, Phys. Rev. B **1**, 2362 (1970).
[22] J. CAZAUX and P. GRAMARI, J. Physique **38**, L133 (1977).
[23] B. L. HENKE, E. M. GULLIKSON, and J. C. DAVIS, At. Data Nucl. Data Tab. **54**, No. 2 (1993).
[24] W. BRANDT, in: Atomic Collisions in Solids, Eds. S. DATZ, B. R. APPLETON, and C. D. MOAK, Plenum Press, New York 1975 (p. 261).